

# Uncertain Quantum Critical Metrology: From Single to Multi Parameter Sensing

George Mihailescu <sup>1,2,\*</sup> Steve Campbell <sup>1,2,3,†</sup> and Karol Gietka <sup>4,‡</sup>

<sup>1</sup>*School of Physics, University College Dublin, Belfield, Dublin 4, Ireland*

<sup>2</sup>*Centre for Quantum Engineering, Science, and Technology, University College Dublin, Dublin 4, Ireland*

<sup>3</sup>*Dahlem Center for Complex Quantum Systems, Freie Universität Berlin, 14195 Berlin, Germany*

<sup>4</sup>*Institut für Theoretische Physik, Universität Innsbruck, Technikerstraße 21a, A-6020 Innsbruck, Austria*

(Dated: July 30, 2024)

Critical quantum metrology relies on the extreme sensitivity of a system's eigenstates near the critical point of a quantum phase transition to Hamiltonian perturbations. This means that these eigenstates are extremely sensitive to *all* the parameters of the Hamiltonian. In practical settings, there always exists a degree of experimental uncertainty in the control parameters—which are approximately known quantities. Despite such uncertainties representing the most relevant source of noise in critical metrology, their impact on the attainable precision has been largely overlooked. In this work we present a general framework, interpolating between the single and multi-parameter estimation settings, allowing for the proper bookkeeping of relevant errors. We apply this framework to the paradigmatic transverse field Ising and Lipkin-Meshkov-Glick models, explicitly showing how uncertainty in control parameters impacts the sensitivity of critical sensors. For finite-size systems, we establish that there exists a trade-off between the amount of uncertainty a many-body probe can withstand while still maintaining a quantum advantage in parameter estimation.

*Introduction.*—Critical quantum metrology [1–3] aims to leverage the increased sensitivity to parameter variations for a system close to a quantum phase transition (QPT) in order to achieve high precision measurements [4–24]. This can be quantified by directly translating the sensitivity of Hamiltonian parameters to be estimated through the Cramér-Rao bound, which relates the quantum Fisher information (QFI) with the estimation uncertainty [25]. When the parameter of interest can be related to the relevant order parameter of the QPT, such increased sensitivity can be achieved. However, an important caveat is that all other parameters of the problem must be precisely known for the framework of single parameter estimation theory to be applicable. In general, this assumption is rather stringent. Typically, some degree of experimental uncertainty or noise is present [26–28]. In the context of quantum critical systems, while high precision experiments are possible [29], as complexity and system size increase—a requisite for critical quantum many-body systems—the resources required to perfectly control and characterize these systems, such as time, also increase [4, 5, 30]. Furthermore, universality is a hallmark of systems approaching their critical point [31, 32], making the system dependent on many, if not all, Hamiltonian parameters precisely where the expected critical enhancement can be achieved. It is therefore intuitive that any uncertainty in at least one of these parameters is expected to negatively affect the QFI and thus deteriorate any potential quantum advantage. Although the effect of noise on performance of critical sensing has been studied in the literature [5, 19, 21], the impact of the most crucial one—the uncertainty of control parameters—has thus far been largely overlooked.

A more appropriate treatment of critical metrology requires a methodology that relaxes the core constraint of the single parameter framework, i.e., that all parameters are assumed to be perfectly known [33–36]. In addition to providing a more realistic description of the actual achievable precision,

this approach also allows for mitigating the necessity of complex and resource-intensive experimental control, ultimately enabling the identification of regions where a true quantum advantage is achievable. A candidate framework for such a purpose is multiparameter quantum metrology [33, 34, 37–40], where the aim is typically to estimate multiple parameters, in principle simultaneously. Clearly, within this framework, we can still assume there is a central parameter we wish to infer, and additionally, there are other relevant parameters about which we have no *a priori* information. Contextually, in terms of critical metrology, the QPT is driven by a single, experimentally controllable system parameter  $\beta$ , and our objective is to infer the desired system parameter  $\alpha$ . The multi-parameter paradigm represents the situation in which the driving (control) parameter  $\beta$  is unknown. However, typically the driving parameter is an experimentally controllable knob and therefore is known within some finite window of resolution. It should be clear then that the multiparameter paradigm provides us with a worst-case scenario for the estimation of a central desired quantity,  $\alpha$ , whereby we have a complete lack of knowledge regarding the value of the driving parameter,  $\beta$ .

In this work, we present a general approach to quantum parameter estimation, interpolating between the two extreme scenarios of single and multi-parameter estimation, allowing for the proper bookkeeping of relevant errors [8, 35, 41]. We apply this formalism to quantum critical metrology and investigate how uncertainties in the driving parameter influence the ability to infer an unknown parameter and whether a relevant advantage is maintained. We consider the Ising and Lipkin-Meshkov-Glick models as two paradigmatic critical systems, showing that the multiparameter estimation framework predicts a catastrophic failure in the sensing capabilities of the probe in these models. By allowing for a degree of statistical uncertainty in the driving parameter, our framework demonstrates that a quantum advantage can still be achieved with critical probes even in the presence of such uncertainties.

*Parameter estimation in the presence of uncertainties.*—In the most general quantum sensing scenario, there are a set of unknown parameters  $\vec{x}$  to be estimated through suitable measurements of a quantum probe [42–44]. Information regarding this set of parameters is encoded in the state of the probe, given by the density matrix  $\hat{\rho}(\vec{x}) = \sum_i \lambda_i |\lambda_i\rangle \langle \lambda_i|$ , with  $\lambda_i$  being the probability of the probe to occupy state  $|\lambda_i\rangle$  which depends on  $\vec{x}$ . This information is determined by performing a large number of measurements. The precision of parameter estimation is given by the quantum Cramér-Rao bound [25] (hat notation indicates a matrix):

$$\text{Cov}[\vec{x}] \geq \hat{I}^{-1}, \quad (1)$$

which is an element-wise matrix inequality, lower bounding the precision of parameter estimation through the covariance matrix. The elements are  $\text{Cov}(\alpha, \beta) = \langle (\alpha - \langle \alpha \rangle)(\beta - \langle \beta \rangle) \rangle$ , where  $\alpha$  and  $\beta$  label parameters from  $\vec{x}$ . Entries of the quantum Fisher information matrix (QFIM) are given by:

$$\mathcal{I}_{\alpha\beta} = \sum_{i,j} \frac{2 \text{Re} [\langle \lambda_i | \partial_\alpha \hat{\rho} | \lambda_j \rangle \langle \lambda_j | \partial_\beta \hat{\rho} | \lambda_i \rangle]}{\lambda_i + \lambda_j}, \quad (2)$$

where diagonal elements relate to the single parameter precision and are obtained by suitably maximizing over all possible positive operator-valued measures. The off-diagonal elements relate to the correlation between parameters. For pure states, the QFIM may be simplified to:

$$\mathcal{I}_{\alpha\beta} = 4 \text{Re} [\langle \partial_\alpha \psi | \partial_\beta \psi \rangle - \langle \partial_\alpha \psi | \psi \rangle \langle \psi | \partial_\beta \psi \rangle]. \quad (3)$$

It is informative to consider the simple case where we have two parameters to be estimated, although the results readily extend to an arbitrary number of variables. From Eq. (1), the attainable precision with respect to parameter  $\alpha$  is given by:

$$\Delta\alpha \geq \frac{\mathcal{I}_{\beta\beta}}{\mathcal{I}_{\alpha\alpha}\mathcal{I}_{\beta\beta} - \mathcal{I}_{\alpha\beta}\mathcal{I}_{\beta\alpha}}. \quad (4)$$

To contrast this, in the single parameter setting where  $\beta$  is assumed to be known precisely (equivalently  $\mathcal{I}_{\beta\alpha} = \mathcal{I}_{\alpha\beta} = 0$ ), Eq. (4) reduces to  $\Delta\alpha \geq 1/\mathcal{I}_{\alpha\alpha}$ . As the QFIM is a positive semi-definite matrix, it follows from Eq. (4) that the precision in single parameter estimation is lower bounded by the multi-parameter counterpart [34]. Thus, while the single-parameter estimation framework gives an optimistic lower bound on the precision, the multi-parameter case gives a pessimistic one. This becomes particularly evident when considering cases where the parameters of interest are related to one another. From Eq. (4), it is clear that in order for the multiparameter problem to be well posed, the QFIM must be an invertible quantity [45, 46], requiring that:

$$\det \hat{I} = \mathcal{I}_{\alpha\alpha}\mathcal{I}_{\beta\beta} - \mathcal{I}_{\alpha\beta}^2 \neq 0. \quad (5)$$

Thus, when the QFIM is singular, i.e.,  $\det \hat{I} = 0$ , the quantum Cramér-Rao bound is not well defined, essentially implying

that the lowest possible uncertainty for estimating a parameter is infinite. Often, the presence of the singularity can be interpreted as indicating that we are not inferring distinct parameters  $\alpha$  and  $\beta$ , but rather an effective ratio,  $\alpha/\beta$  [46]. In critical metrology, this becomes particularly relevant since the aim is to leverage the sudden change in Hamiltonian parameters near the critical point. However, at the critical point, the ground state depends on many, if not all, system parameters, making it apparent that the lack of knowledge about any system parameters other than the central parameter of interest may lead to a complete loss of metrological utility.

In most relevant settings, control parameters are implemented with a given tolerance, making it more meaningful to consider bounding the attainable precision on  $\alpha$  when  $\beta$  is known within some finite interval of resolution. In full generality, we may model the sensitivity to parameter  $\alpha$  given some uncertainty in the driving parameter  $\beta$  by introducing a probability distribution,  $p(\beta)$ , obtained from sampling the generated states for a given value of  $\beta$ . Formally, this can be achieved by considering the probe state as an infinite mixture of states, each corresponding to a different value of  $\beta$ . The corresponding sensitivity is then given by evaluating the effective single parameter QFI for this family of states, thereby explicitly accounting for imprecision or fluctuations in  $\beta$ .

Critical metrology achieves increased sensitivity in parameter estimation by exploiting properties of eigen states near the critical point of QPTs, and the optimal sensitivity is quantified using Eq. (3). However, as we are dealing with a mixture of states—specifically a mixture of ground states—we require the ground state density matrix for a given choice of  $\beta$ , defined as  $\hat{\rho}(\alpha, \beta) = |\psi_{GS}\rangle \langle \psi_{GS}|$ . To sample the corresponding quantum state for a given choice of  $\beta$ , we then weigh the ground state density matrix according to the probability distribution  $p(\beta)$ . A natural choice is a Gaussian distribution, such that  $p(\beta) = \frac{1}{\sigma\sqrt{2\pi}} \exp\left\{-\frac{1}{2}\left(\frac{\beta-\bar{\beta}}{\sigma}\right)^2\right\}$ , yielding on average a final state of the form:

$$\hat{\rho}(\alpha, \sigma) = \int_{-\infty}^{\infty} d\beta \frac{\exp\left\{-\frac{1}{2}\left(\frac{\beta-\bar{\beta}}{\sigma}\right)^2\right\}}{\sigma\sqrt{2\pi}} \hat{\rho}(\alpha, \beta), \quad (6)$$

with  $\bar{\beta}$  the average value of parameter  $\beta$ , and  $\sigma$  the variance quantifying the (im)precision. The corresponding sensitivity is then obtained from the QFI of the averaged state using Eq. (2), which we denote as  $\bar{\mathcal{I}}_{\alpha\alpha}$ . This scenario represents an interpolation between the various relevant settings. For  $\sigma \rightarrow 0$ , we recover the single parameter estimation case where  $\beta$  is assumed to be precisely known; while  $\sigma \rightarrow \infty$  corresponds to the multi-parameter setting where  $\beta$  is unknown and, depending on the specific setting at hand, the QFIM may become singular.

*Applications.*—We apply our framework to the general class of Hamiltonians given by:

$$\hat{H} = \omega \sum_i^N \hat{\sigma}_i^z - \sum_{i \neq j=1}^N g_{ij} \hat{\sigma}_i^x \hat{\sigma}_j^x \quad (7)$$

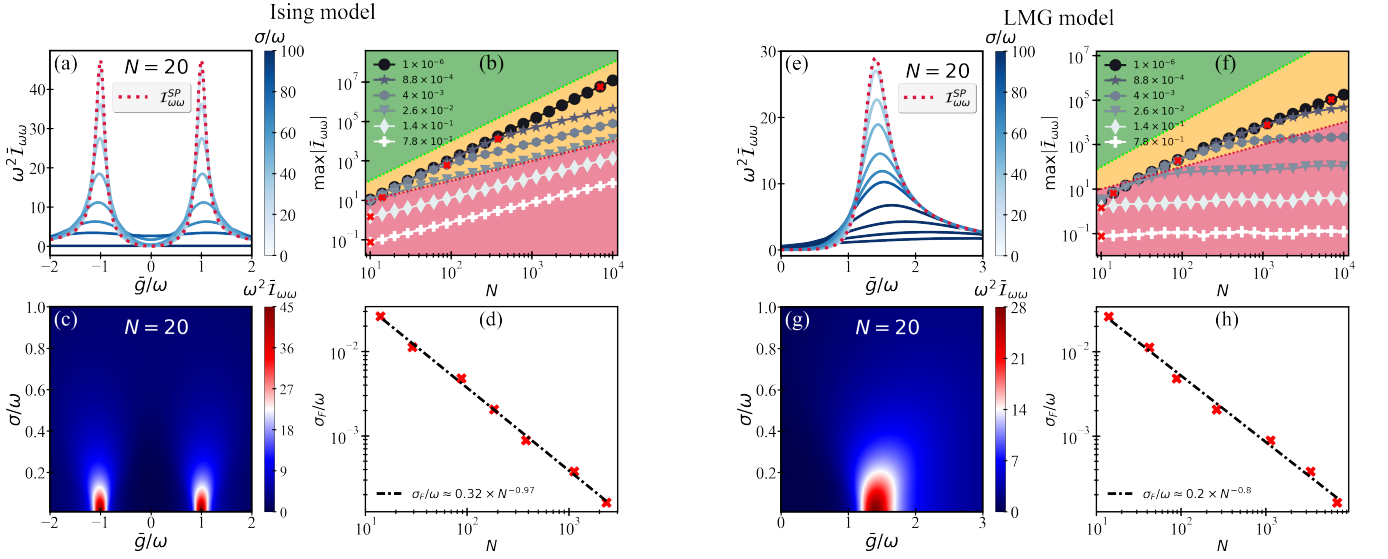


FIG. 1. Left panel: *Ising model*. Right panel: *LMG model*. Sensitivity to the bare frequency  $\omega$  with uncertainty in the coupling  $g$  quantified by  $\sigma/\omega$ . In (a) and (c) as well as (e) and (g) the attainable sensitivity to the frequency  $\omega$  is shown for various degrees of uncertainty for  $N = 20$  spins. In (a) and (e), the dotted red line shows the ideal sensitivity  $\mathcal{I}_{\omega\omega}^{SP}$  of the single parameter case when  $g$  is perfectly known. Solid lines show attainable sensitivity for a given precision in  $g$ . (c) and (g) depict the full phase diagram for parameter sensitivity. (b) and (f) show scaling of the peak QFI with a given uncertainty,  $\bar{\mathcal{I}}_{\omega\omega}$ , in the coupling  $g$  as a function of system size  $N$ . (d) and (h) depict the maximal uncertainty at which the QFI feels the uncertainty of the control parameter  $g$  as a function of system size  $N$ .

with a transverse field  $\omega$  that we wish to estimate and  $g_{ij}$  the interaction strength between the  $i^{\text{th}}$  and  $j^{\text{th}}$  spin, which we assume is controllable. We will consider two paradigmatic examples of the above: the transverse field Ising model (TFIM) when  $g_{ij} = g$  is non-zero only for the nearest neighbors [47, 48], and the Lipkin-Meshkov-Glick (LMG) model when  $g_{ij} = g/N$  [49–53] (see also Appendix A for a toy-model Landau-Zener Hamiltonian). In both cases, it should be immediately evident that one can perform a simple rescaling of the Hamiltonian, and therefore the ground state will be dependent on the parameters' ratio, immediately implying that the QFIM is singular [34].

Explicitly, for the Ising limit assuming periodic boundary conditions, by utilizing a Jordan-Wigner mapping and transforming to momentum space, we can obtain an exact expression for the ground state of the many-body system,  $|\psi_{GS}\rangle_N = \bigotimes_{k>0} |\psi_{GS}\rangle_k$ , where  $|\psi_{GS}\rangle_k = \cos \theta_k/2 |0\rangle_k + \sin \theta_k/2 |1\rangle_k$  (see Appendix B for details). Exploiting this and leveraging the fact that the QFI is additive under a tensor product, such that  $\hat{\mathcal{I}}_{\omega\omega} [|\psi_{GS}\rangle_N] = \hat{\mathcal{I}}_{\omega\omega} [|\psi_{GS}\rangle_{k1}] + \hat{\mathcal{I}}_{\omega\omega} [|\psi_{GS}\rangle_{k2}] + \dots + \hat{\mathcal{I}}_{\omega\omega} [|\psi_{GS}\rangle_{kN}]$ , we obtain a closed-form expression for the QFIM

$$\hat{\mathcal{I}}_{\text{Ising}} = \sum_k \begin{pmatrix} \frac{g^2 \sin^2 k}{(g^2 + \omega^2 - 2g\omega \cos k)^2} & -\frac{g\omega \sin^2 k}{(g^2 + \omega^2 - 2g\omega \cos k)^2} \\ -\frac{g\omega \sin^2 k}{(g^2 + \omega^2 - 2g\omega \cos k)^2} & \frac{\omega^2 \sin^2 k}{(g^2 + \omega^2 - 2g\omega \cos k)^2} \end{pmatrix}, \quad (8)$$

with  $k = \pi(2n + 1)/N$  and  $n = 0, 1, 2, \dots, N/2 - 1$ , which is clearly singular for all  $N$ , irrespective of the distance to the critical point. Consequently, the estimation of the bare frequency  $\omega$  is strictly prohibited when the coupling  $g$  is un-

known. The single-parameter sensitivity to the bare frequency  $\omega$  corresponds to the first element of Eq. (8).

Allowing for uncertainty in the coupling, we construct a mixture of ground states sampled for a given value of  $g$  according to Eq. (6). In Fig. 1, we show the QFI for this averaged state, denoted  $\bar{\mathcal{I}}_{\omega\omega}$ , for the TFIM. Moreover, in Fig. 1(a), we explicitly compare the ideal single-parameter sensitivity,  $\mathcal{I}_{\omega\omega}$  shown in the dotted red line, with attainable sensitivity for a given uncertainty, in the range  $\sigma/\omega = [0, 100]$  from solid light blue to solid dark blue for  $N = 20$  spins. Crucially, we note that for small uncertainty in  $g$ , the QFI retains the peak of the single-parameter case, and this peak sensitivity decreases as our uncertainty in  $g$  increases. Notably, in the limit  $\sigma \rightarrow \infty$ , uncertainty in the coupling completely deteriorates sensitivity to the bare frequency  $\omega$ , recovering the expected multi-parameter result when the QFIM is singular. Fig. 1(c) shows the full phase diagram of the QFI for  $N = 20$  spins as a function of the variance,  $\sigma/\omega$ , where we clearly see that introducing uncertainty in our knowledge of the coupling strength reduces and smooths out the peak sensitivity.

In the best-case scenario when the coupling  $g$  is perfectly known, the peak sensitivity at the critical point  $g = \omega$  as a function of system size scales as  $(N^2 + N)/8\omega^2$ . Herein lies the power of critical quantum metrology, whereby treating the system size  $N$  as a resource for sensing, the QFI scales as  $N^\gamma$  with an exponent which is typically  $\gamma > 1$  with respect to parameter(s) which drive the phase transition. Such scaling represents an advantage over the independent (non-interacting) case where  $\gamma = 1$ . An important consideration is therefore if such an advantage is indeed attainable in the

presence of relevant experimental imprecision. In Fig. 1(b), we plot the scaling of the QFI in the presence of uncertainty,  $\tilde{\mathcal{I}}_{\omega\omega}$  as a function of system size  $N$  for various degrees of imprecision in the control parameter  $g$ . The red region indicates scaling that is worse than linear ( $\gamma < 1$ ), the yellow region indicates scaling better than linear but worse than quadratic ( $2 > \gamma > 1$ ), and the green region indicates better than quadratic scaling ( $\gamma > 2$ ). The red crosses indicate the point at which the QFI is affected by the imprecision: specifically, when the QFI no longer scales as in the ideal scenario when  $g$  is known with absolute certainty,  $(N^2 + N)/8\omega^2$ . Importantly, we note from the red crosses that larger system sizes are less robust to relevant uncertainties—indicating an important experimental trade-off between attainable sensitivity endowed by larger system sizes and their robustness to relevant perturbations. This provides a crucial practical consideration in the design of criticality-enhanced sensors, whereby there is an optimal trade-off between the sensitivity offered by larger systems and their robustness to uncertainties. Furthermore, treating the definition of criticality to hold strictly for an infinite system, we note that in the asymptotic limit of system size any finite perturbation or uncertainty would necessarily prohibit scaling larger than  $\gamma = 1$ , leading to a constant factor improvement, consistent with Ref. [54]. Fig. 1(d) depicts the maximal uncertainty at which the QFI *feels* the uncertainty of the control parameter  $g$ —the red crosses from (b), denoted  $\sigma_F/\omega$ , as a function of system size  $N$  [for clarity we do not show all the generated data in (b), hence there are more red crosses in (d) than in (b)]. For more details, see Appendix C]. From here we can see that smaller system sizes are more robust to the uncertainty than bigger systems. According to a numerical fit,  $\sigma_F/\omega \approx 0.32 \times N^{-0.97}$  in the TFIM, indicating how precisely the control parameter  $g$  has to be known as a function of  $N$  to retain the same sensitivity as in the single-parameter paradigm.

A qualitatively similar behavior can be demonstrated for the LMG model. The isometric all-to-all coupling means it is convenient to recast Eq. (7) in terms of collective spin operators,  $\hat{S}_i \equiv \sum_n \hat{\sigma}_i^n / 2$  with  $i \in \{x, y, z\}$  [41],

$$\hat{H} = \omega \hat{S}_z - \frac{g}{N} \hat{S}_x^2. \quad (9)$$

The LMG Hamiltonian experiences a second order QPT in the thermodynamic limit at  $g = g_c = \omega$  [55]. This can be explicitly seen by using the Holstein-Primakoff transformation and applying the  $N \rightarrow \infty$  approximation,

$$\hat{H} = \omega \hat{a}^\dagger \hat{a} - \frac{g}{4} (\hat{a}^\dagger + \hat{a})^2. \quad (10)$$

In the thermodynamic limit, the eigenstates are squeezed Fock states of the non-interacting system  $|n_\xi\rangle = \hat{S}(\xi)|n\rangle$ , where  $\hat{S}(\xi) = \exp\left\{\frac{1}{2}(\xi^* \hat{a}^2 - \xi \hat{a}^{\dagger 2})\right\}$  is the squeezing operator and  $\xi = \frac{1}{4} \ln\{1 - g/\omega\}$  is the squeezing parameter. At the critical point, the eigenstates become infinitely squeezed, which is responsible for the non-analytic behavior at the critical

point [56], while for finite-sized systems, this non-analytic behavior is smoothed out as a function of  $N$  [57].

Since in the thermodynamic limit the ground state is completely defined by the squeezing parameter  $\xi$ , the QFIM can be simply expressed as,

$$\begin{aligned} \hat{\mathcal{I}}_{\text{LMG}} &= 2 \begin{pmatrix} [\partial_\omega \xi]^2 & [\partial_\omega \xi][\partial_g \xi] \\ [\partial_\omega \xi][\partial_g \xi] & [\partial_g \xi]^2 \end{pmatrix} \\ &= \frac{1}{32} \begin{pmatrix} \frac{\omega^2}{(\omega-g)^2 \omega^2} & \frac{g\omega}{(\omega-g)^2 \omega^2} \\ \frac{g\omega}{(\omega-g)^2 \omega^2} & \frac{g^2}{(\omega-g)^2 \omega^2} \end{pmatrix}, \end{aligned} \quad (11)$$

which, again due to the fact that the ground state depends on the ratio of parameters, is evidently singular regardless of the distance to the critical point. In order to calculate the QFI matrix elements for a finite-size system including uncertainties in the control parameter  $g$ , we resort to using numerical calculations. The uncertainty of the control parameter  $g$  is incorporated in the same way as for the TFIM. The exemplary QFI with respect to  $\omega$  for  $N = 20$  spins is presented in Fig. 1(e) and the corresponding full phase diagram in the presence of uncertainty in Fig. 1(g). We also plot the maximal attainable QFI as a function of the system size for various levels of uncertainty in the control parameter [see Fig. 1(f)]. Interestingly, although the LMG model is an all-to-all interacting system, the QFI scales less than quadratically as in the case of nearest-neighbor interacting TFIM,  $\gamma = 4/3$ . Similar to the TFIM, we also notice that for every  $N$  there exists a corresponding  $\sigma_F/\omega$  at which the QFI stops following the ideal case single-parameter scaling, denoted by the red crosses. The numerical fit reveals that  $\sigma_F/\omega \approx 0.2 \times N^{-0.8}$ , shown in Fig. 1(h).

*Conclusions.*—In this work, we have developed a framework to characterize the effectiveness of critical quantum probes, taking into account inherent uncertainties in other parameters of the model which we expect to be the most serious obstacle for achieving quantum enhancement in critical sensing. We demonstrate that this framework interpolates between the best and worst-case scenarios, as captured by single and multiparameter estimation settings. While the power of critical quantum probes typically lies in the scaling of the quantum Fisher information with respect to system size  $N$ , we reveal that practical settings involving relevant uncertainties exhibit a fundamental trade-off between the sensitivity offered by larger system sizes and their robustness to imprecision. Furthermore, we show that in the asymptotic limit of system size, any finite perturbation negates the advantage in quantum Fisher information scaling.

We applied our framework to two paradigmatic spin systems: the Lipkin-Meshkov-Glick model and the Transverse Field Ising Model. In doing so, we also provided an analytical approach for determining the quantum Fisher information matrix and its determinant for any system that can be mapped to free fermions. Therefore, we anticipate that our results can be extended to a wide range of other spin systems, such as  $XY$ ,  $XXZ$  models, and topological systems like the Su-Schrieffer-Heeger and Chern models [58].

For the models explicitly considered, we have shown that for every system size, there exists a range of uncertainties in the control parameters for which the predicted critical enhancement of metrological utility in the scaling of quantum Fisher information can be maintained. Our results demonstrate that, in critical metrology, while uncertainty in the precise value of other model parameters will ultimately limit the maximal precision with which the parameter of interest can be determined, a useful quantum advantage can still be achieved. This establishes that, even in the presence of such uncertainties, critical systems remain viable probes for quantum-enhanced sensing tasks.

The authors are grateful to Victor Montenegro, Chiranjib Mukhopadhyay, and Andrew Mitchell for fruitful discussions and thank the organizers of QUMINOS. G.M. acknowledges support from Equal1 Laboratories Ireland Limited. SC acknowledges support from the John Templeton Foundation Grant ID 62422 and the Alexander von Humboldt Foundation. K.G. was supported by the Lise-Meitner Fellowship M3304-N of the Austrian Science Fund (FWF).

---

\* [george.mihailescu@ucdconnect.ie](mailto:george.mihailescu@ucdconnect.ie)

† [steve.campbell@ucd.ie](mailto:steve.campbell@ucd.ie)

‡ [karol.gietka@uibk.ac.at](mailto:karol.gietka@uibk.ac.at)

- [1] L. Campos Venuti and P. Zanardi, Quantum Critical Scaling of the Geometric Tensors, *Phys. Rev. Lett.* **99**, 095701 (2007).
- [2] P. Zanardi, P. Giorda, and M. Cozzini, Information-Theoretic Differential Geometry of Quantum Phase Transitions, *Phys. Rev. Lett.* **99**, 100603 (2007).
- [3] P. Zanardi, M. G. A. Paris, and L. Campos Venuti, Quantum criticality as a resource for quantum estimation, *Phys. Rev. A* **78**, 042105 (2008).
- [4] M. M. Rams, P. Sierant, O. Dutta, P. Horodecki, and J. Zakrzewski, At the Limits of Criticality-Based Quantum Metrology: Apparent Super-Heisenberg Scaling Revisited, *Phys. Rev. X* **8**, 021022 (2018).
- [5] L. Garbe, M. Bina, A. Keller, M. G. A. Paris, and S. Felicetti, Critical Quantum Metrology with a Finite-Component Quantum Phase Transition, *Phys. Rev. Lett.* **124**, 120504 (2020).
- [6] S. Wald, S. V. Moreira, and F. L. Semião, In- and out-of-equilibrium quantum metrology with mean-field quantum criticality, *Phys. Rev. E* **101**, 052107 (2020).
- [7] S. S. Mirkhalaf, D. Benedicto Orenes, M. W. Mitchell, and E. Witkowska, Criticality-enhanced quantum sensing in ferromagnetic Bose-Einstein condensates: Role of readout measurement and detection noise, *Phys. Rev. A* **103**, 023317 (2021).
- [8] V. Montenegro, U. Mishra, and A. Bayat, Global Sensing and Its Impact for Quantum Many-Body Probes with Criticality, *Phys. Rev. Lett.* **126**, 200501 (2021).
- [9] K. Gietka, L. Ruks, and T. Busch, Understanding and Improving Critical Metrology. Quenching Superradiant Light-Matter Systems Beyond the Critical Point, *Quantum* **6**, 700 (2022).
- [10] V. P. Pavlov, D. Porras, and P. A. Ivanov, Quantum metrology with critical driven-dissipative collective spin system, *Phys. Scr.* **98**, 095103 (2023).
- [11] T. Ilias, D. Yang, S. F. Huelga, and M. B. Plenio, Criticality-Enhanced Quantum Sensing via Continuous Measurement, *PRX Quantum* **3**, 010354 (2022).
- [12] L. Garbe, O. Abah, S. Felicetti, and R. Puebla, Critical quantum metrology with fully-connected models: from Heisenberg to Kibble-Zurek scaling, *Quantum Sci. Technol.* **7**, 035010 (2022).
- [13] K. Gietka and H. Ritsch, Squeezing and Overcoming the Heisenberg Scaling with Spin-Orbit Coupled Quantum Gases, *Phys. Rev. Lett.* **130**, 090802 (2023).
- [14] R. Salvia, M. Mehboudi, and M. Perarnau-Llobet, Critical Quantum Metrology Assisted by Real-Time Feedback Control, *Phys. Rev. Lett.* **130**, 240803 (2023).
- [15] R. Di Candia, F. Minganti, K. V. Petrovnin, G. S. Paraoanu, and S. Felicetti, Critical parametric quantum sensing, *npj Quantum Inf.* **9**, 23 (2023).
- [16] M. Yu, H. C. Nguyen, and S. Nimmrichter, Criticality-enhanced precision in phase thermometry (2023), [arXiv:2311.14578](https://arxiv.org/abs/2311.14578).
- [17] R. Salvia, M. Mehboudi, and M. Perarnau-Llobet, Critical Quantum Metrology Assisted by Real-Time Feedback Control, *Phys. Rev. Lett.* **130**, 240803 (2023).
- [18] C. Hotter, H. Ritsch, and K. Gietka, Combining Critical and Quantum Metrology, *Phys. Rev. Lett.* **132**, 060801 (2024).
- [19] L. Ostermann and K. Gietka, Temperature-enhanced critical quantum metrology, *Phys. Rev. A* **109**, L050601 (2024).
- [20] G. Mihailescu, A. Kiely, and A. K. Mitchell, Quantum sensing with nanoelectronics: Fisher information for an adiabatic perturbation (2024), [arXiv:2406.18662](https://arxiv.org/abs/2406.18662).
- [21] U. Alushi, W. Górecki, S. Felicetti, and R. Di Candia, Optimality and Noise Resilience of Critical Quantum Sensing, *Phys. Rev. Lett.* **133**, 040801 (2024).
- [22] R. Zhang, W. Ding, Z. Zhang, L. Shao, Y. Zhang, and X. Wang, Relations between quantum metrology and criticality in general  $su(1,1)$  systems, *Phys. Rev. A* **110**, 012413 (2024).
- [23] G. Zicari, M. Carlesso, A. Trombettoni, and M. Paternostro, Criticality-amplified quantum probing of a spontaneous collapse model (2024), [arXiv:2407.09304](https://arxiv.org/abs/2407.09304).
- [24] U. Alushi, A. Coppo, V. Brosco, R. D. Candia, and S. Felicetti, Collective quantum enhancement in critical quantum sensing (2024), [arXiv:2407.18055](https://arxiv.org/abs/2407.18055).
- [25] S. L. Braunstein and C. M. Caves, Statistical distance and the geometry of quantum states, *Phys. Rev. Lett.* **72**, 3439 (1994).
- [26] B. M. Escher, R. L. de Matos Filho, and L. Davidovich, Quantum Metrology for Noisy Systems, *Braz. J. Phys.* **41**, 229 (2011).
- [27] S. Zhou, M. Zhang, J. Preskill, and L. Jiang, Achieving the Heisenberg limit in quantum metrology using quantum error correction, *Nat. Commun.* **9**, 78 (2018).
- [28] P. Yin, X. Zhao, Y. Yang, Y. Guo, W.-H. Zhang, G.-C. Li, Y.-J. Han, B.-H. Liu, J.-S. Xu, G. Chiribella, G. Chen, C.-F. Li, and G.-C. Guo, Experimental super-Heisenberg quantum metrology with indefinite gate order, *Nat. Phys.* **19**, 1122 (2023).
- [29] D. Ding, Z. Liu, B. Shi, G. Guo, K. Mølmer, and C. S. Adams, Enhanced metrology at the critical point of a many-body Rydberg atomic system, *Nat. Phys.* **18**, 1447 (2022).
- [30] K. Gietka, F. Metz, T. Keller, and J. Li, Adiabatic critical quantum metrology cannot reach the Heisenberg limit even when shortcuts to adiabaticity are applied, *Quantum* **5**, 489 (2021).
- [31] M. Heyl, Scaling and Universality at Dynamical Quantum Phase Transitions, *Phys. Rev. Lett.* **115**, 140602 (2015).
- [32] M.-J. Hwang, R. Puebla, and M. B. Plenio, Quantum Phase Transition and Universal Dynamics in the Rabi Model, *Phys. Rev. Lett.* **115**, 180404 (2015).
- [33] G. D. Fresco, B. Spagnolo, D. Valenti, and A. Carollo, Multiparameter quantum critical metrology, *SciPost Phys.* **13**, 077 (2022).
- [34] G. Mihailescu, A. Bayat, S. Campbell, and A. K. Mitchell, Mul-

- tiparameter critical quantum metrology with impurity probes, *Quantum Sci. Technol.* **9**, 035033 (2024).
- [35] W. Górecki and R. Demkowicz-Dobrzański, Multiparameter quantum metrology in the Heisenberg limit regime: Many-repetition scenario versus full optimization, *Phys. Rev. A* **106**, 012424 (2022).
- [36] S. Mondal, A. Sahoo, U. Sen, and D. Rakshit, *Multicritical quantum sensors driven by symmetry-breaking* (2024), [arXiv:2407.14428](https://arxiv.org/abs/2407.14428).
- [37] S. Ragy, M. Jarzyna, and R. Demkowicz-Dobrzański, Compatibility in multiparameter quantum metrology, *Phys. Rev. A* **94**, 052108 (2016).
- [38] J. Liu, H. Yuan, X.-M. Lu, and X. Wang, Quantum Fisher information matrix and multiparameter estimation, *J. Phys. A: Math. Theor.* **53**, 023001 (2019).
- [39] J. Naikoo, R. W. Chhajlany, and J. Kołodyński, Multiparameter Estimation Perspective on Non-Hermitian Singularity-Enhanced Sensing, *Phys. Rev. Lett.* **131**, 220801 (2023).
- [40] R. Kaubruegger, A. Shankar, D. V. Vasilyev, and P. Zoller, Optimal and Variational Multiparameter Quantum Metrology and Vector-Field Sensing, *PRX Quantum* **4**, 020333 (2023).
- [41] G. Salvatori, A. Mandarino, and M. G. A. Paris, Quantum metrology in Lipkin-Meshkov-Glick critical systems, *Phys. Rev. A* **90**, 022111 (2014).
- [42] V. Giovannetti, S. Lloyd, and L. Maccone, Quantum Metrology, *Phys. Rev. Lett.* **96**, 010401 (2006).
- [43] V. Giovannetti, S. Lloyd, and L. Maccone, Advances in quantum metrology, *Nat. Photon.* **5**, 222 (2011).
- [44] J. Liu, H. Yuan, X.-M. Lu, and X. Wang, Quantum fisher information matrix and multiparameter estimation, *J. Phys. A: Math. Theor.* **53**, 023001 (2019).
- [45] P. Stoica and T. Marzetta, Parameter estimation problems with singular information matrices, *IEEE Trans. Signal Process.* **49**, 87 (2001).
- [46] A. Z. Goldberg, J. L. Romero, A. S. Sanz, and L. L. Sánchez-Soto, Taming singularities of the quantum Fisher information, *Int. J. Quantum Inf.* **19**, 2140004 (2021).
- [47] P. Pfeuty, The one-dimensional Ising model with a transverse field, *Ann. Phys.* **57**, 79 (1970).
- [48] R. B. Stinchcombe, Ising model in a transverse field. i. Basic theory, *J. Phys. C: Solid State Phys.* **6**, 2459 (1973).
- [49] H. Lipkin, N. Meshkov, and A. Glick, Validity of many-body approximation methods for a solvable model: (i). Exact solutions and perturbation theory, *Nucl. Phys.* **62**, 188 (1965).
- [50] T. Zibold, E. Nicklas, C. Gross, and M. K. Oberthaler, Classical Bifurcation at the Transition from Rabi to Josephson Dynamics, *Phys. Rev. Lett.* **105**, 204101 (2010).
- [51] Z. Li, B. Braverman, S. Colombo, C. Shu, A. Kawasaki, A. F. Adiyatullin, E. Pedrozo-Peñañiel, E. Mendez, and V. Vuletić, Collective Spin-Light and Light-Mediated Spin-Spin [i]nteractions in an Optical Cavity, *PRX Quantum* **3**, 020308 (2022).
- [52] J. A. Muniz, D. Barberena, R. J. Lewis-Swan, D. J. Young, J. R. K. Cline, A. M. Rey, and J. K. Thompson, Exploring dynamical phase transitions with cold atoms in an optical cavity, *Nature* **580**, 602 (2020).
- [53] Z. Li, S. Colombo, C. Shu, G. Velez, S. Pilatowsky-Cameo, R. Schmied, S. Choi, M. Lukin, E. Pedrozo-Peñañiel, and V. Vuletić, Improving metrology with quantum scrambling, *Science* **380**, 1381 (2023).
- [54] R. Demkowicz-Dobrzański, J. Kołodyński, and M. Guță, The elusive Heisenberg limit in quantum-enhanced metrology, *Nat. Commun.* **3**, 1063 (2012).
- [55] P. Ribeiro, J. Vidal, and R. Mosseri, Thermodynamical limit of the Lipkin-Meshkov-Glick Model, *Phys. Rev. Lett.* **99**, 050402 (2007).
- [56] K. Gietka, Squeezing by critical speeding up: Applications in quantum metrology, *Phys. Rev. A* **105**, 042620 (2022).
- [57] S. Dusuel and J. Vidal, Finite-size scaling exponents of the lipkin-meshkov-glick model, *Phys. Rev. Lett.* **93**, 237204 (2004).
- [58] S. Sarkar, C. Mukhopadhyay, A. Alase, and A. Bayat, Free-Fermionic Topological Quantum Sensors, *Phys. Rev. Lett.* **129**, 090503 (2022).
- [59] C. Zener, Non-adiabatic crossing of energy levels, *Proc. Math. Phys. Eng.* **137**, 696 (1932).
- [60] J. Zhang, F. M. Cucchietti, C. M. Chandrashekar, M. Laforest, C. A. Ryan, M. Ditty, A. Hubbard, J. K. Gamble, and R. Laflamme, Direct observation of quantum criticality in Ising spin chains, *Phys. Rev. A* **79**, 012305 (2009).
- [61] L. Innocenti, G. De Chiara, M. Paternostro, and R. Puebla, Ultrafast critical ground state preparation via bang-bang protocols, *New J. Phys.* **22**, 093050 (2020).
- [62] G. Mbeng, A. Russomanno, and G. Santoro, The quantum Ising chain for beginners, *SciPost Phys. Lect. Notes* , 82 (2024).

## APPENDIX A: QUANTUM FISHER INFORMATION MATRIX FOR LANDAU-ZENER TOY-MODEL

The Landau-Zener model [59] describes a two-level system in a control field  $g$ ,

$$\hat{H}_{LZ} = \frac{\omega}{2}\hat{\sigma}_z - \frac{g}{2}\hat{\sigma}_x. \quad (\text{A1})$$

where  $\omega$  is the level splitting for  $g = 0$ , and  $\hat{\sigma}_i$  is the  $i$ th Pauli matrix. Being a single-particle system, the Landau-Zener model does not exhibit a QPT. However, it features an avoided crossing at  $g = 0$  and can therefore be considered as a toy model for criticality [30, 60, 61]. The instantaneous ground state of the Landau-Zener model is given by,

$$|\psi_0\rangle = -\frac{g + \sqrt{\omega^2 + g^2}}{\sqrt{2g(g + \sqrt{\omega^2 + g^2}) + 2\omega^2}}|\downarrow\rangle \quad (\text{A2})$$

$$+ \frac{\omega}{\sqrt{2g(g + \sqrt{\omega^2 + g^2}) + 2\omega^2}}|\uparrow\rangle. \quad (\text{A3})$$

Using Eq. (3) we can readily obtain the QFI matrix for the above ground state,

$$\hat{I}_{LZ} = \begin{pmatrix} \frac{g^2}{(g^2 + \omega^2)^2} & -\frac{g\omega}{(g^2 + \omega^2)^2} \\ -\frac{\omega g}{(g^2 + \omega^2)^2} & \frac{\omega^2}{(g^2 + \omega^2)^2} \end{pmatrix}. \quad (\text{A4})$$

The above QFI matrix is always singular regardless of the distance to the avoided crossing, i.e.,  $\det[\hat{I}_{LZ}] = I_{\omega\omega}I_{gg} - I_{\omega g}^2 = 0$ . In Fig. A1(a) we show the elements of the QFIM as a function of driving parameter  $g$  when  $\omega = 1$ , with  $I_{\omega\omega}$ ,  $I_{gg}$ , and  $I_{\omega g}$  depicted in the solid blue, dash-dotted red, and dashed grey lines respectively. We note that the quantity  $\omega^2 I_{\alpha\beta}$  is a universal scaling function of the rescaled parameter  $g/\omega$ . In general, we may expect accidental crossings of the elements of the QFIM, in (a) we highlight the coalescence when  $\omega = g = 1$ . We attribute the singularity of the QFIM in the Landau-Zener model to the fact that we are not sensing separately parameters  $\omega$  and  $g$ , but rather, an effective ratio of  $g/\omega$ . As we are sensing an effective ratio of parameters, precisely when  $\omega = g$ , the ratio  $g/\omega = 1$ , and elements of the QFIM attain the same value, and coalesce.

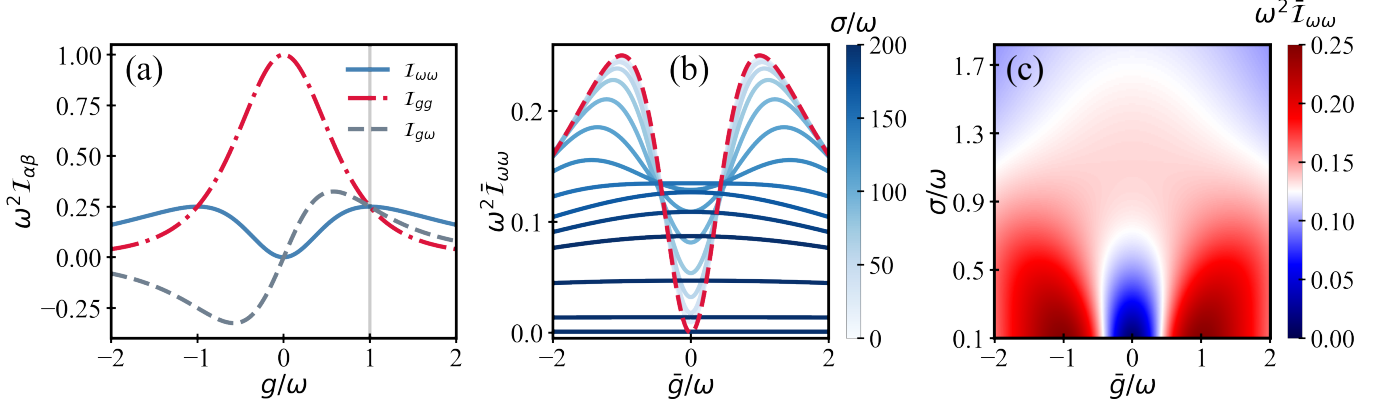


FIG. A1. *Landau-Zener model*: (a) Elements of the QFIM for various  $g$  when the bare frequency  $\omega = 1$ . (b) Sensitivity to the bare frequency  $\omega$  with various degrees of uncertainty in the control parameter  $g$ . The dashed red line shows the ideal sensitivity  $I_{\omega\omega}^{SP}$  of the single parameter scenario when  $g$  is known. The solid blue lines show attainable QFI  $\bar{I}_{\omega\omega}$  with uncertainty in the coupling  $g$ . (c) The full phase diagram in attainable QFI with varying degree of precision quantified by  $\sigma$ .

The multiparameter case represents the scenario when neither the bare frequency  $\omega$  or the driving field  $g$  are known. As in the main text, we investigate the scenario in which we wish to estimate the bare frequency  $\omega$ , but we have some finite window of resolution in the driving parameter  $g$ . This finite window of resolution represents the degree of uncertainty we have, quantified by the variance of a Gaussian distribution  $\sigma$ . The corresponding sensitivity is found viz.,

$$\hat{\varrho}(\omega, \sigma) = \int_{-\infty}^{\infty} dg \frac{\exp\left\{-\frac{1}{2}\left(\frac{g-\bar{g}}{\sigma}\right)^2\right\}}{\sqrt{2\pi\sigma^2}} \hat{\varrho}(\omega, g), \quad (\text{A5})$$

with  $\hat{\rho}(\omega, g)$  the ground state density matrix of Eq. (A2),  $\sigma$  is the variance, and  $\bar{g}$  is the expected value of the driving parameter  $g$ . In Fig. A1 (b) the ideal sensitivity when the control field  $g$  is perfectly known—i.e., the single parameter sensitivity,  $\mathcal{I}_{\omega\omega}^{SP}$ , is shown in the dashed red line. The solid blue lines depict the attainable sensitivity  $\bar{\mathcal{I}}_{\omega\omega}$  for various uncertainty quantified by  $\sigma$ . We note that in the limit  $\sigma \rightarrow \infty$ , when the driving parameter  $g$  is essentially unknown, there is zero attainable sensitivity to the bare frequency  $\omega$ . This is because the  $\sigma \rightarrow \infty$  limit is essentially the multiparameter scenario: as the QFIM is singular, when the driving parameter  $g$  is unknown, the frequency  $\omega$  cannot be inferred. In scenarios where the QFIM is non-singular, we would expect the  $\sigma \rightarrow \infty$  limit to yield some finite sensitivity. In panel (c) we show the full phase diagram for the attainable sensitivity when there is uncertainty in the driving parameter  $g$ .

## APPENDIX B: QUANTUM FISHER INFORMATION MATRIX FOR TRANSVERSE FIELD ISING MODEL

In this section, we provide a simple prescription for finding a closed form solution for the QFIM and determinant of QFIM for any system that can be mapped to free fermions. We present these results by considering the TFIM as a paradigmatic example. The system can be diagonalized by first using the Jordan-Wigner transformation and then going to momentum space to obtain,

$$\hat{H}_k = 2 \sum_k \left( [\omega - g \cos k] [\hat{c}_k^\dagger \hat{c}_k - \hat{c}_{-k}^\dagger \hat{c}_{-k}] - g \sin k [ie^{-2i\phi} \hat{c}_k^\dagger \hat{c}_{-k}^\dagger - ie^{2i\phi} \hat{c}_k \hat{c}_{-k}] \right), \quad (\text{A6})$$

where the arbitrary overall phase,  $\phi$ , was introduced in writing the model in the quasi-momentum  $k$ -space basis. The phase factor,  $\phi$ , simply corresponds to changing the phase of pairs created in momentum space. All Hamiltonian terms now come in momentum space pairs,  $(k, -k)$ , where one can define the full Hamiltonian by considering only the positive momentum  $k$  values, corresponding to  $k = \pi(2n+1)/N$  where  $n = 0, 1, 2, \dots, N/2 - 1$ . As noted in [62], the Hamiltonian's  $\hat{H}_k$  live in a 4-dimensional space spanned by the states  $\{|0\rangle, \hat{c}_k^\dagger |0\rangle, \hat{c}_{-k}^\dagger |0\rangle, \hat{c}_k^\dagger \hat{c}_{-k}^\dagger |0\rangle\}$ , which has a single non-trivial  $2 \times 2$  block. To deal with the necessary combination of states living in these non-trivial blocks, spanned by  $\{|0\rangle, \{\hat{c}_k^\dagger \hat{c}_{-k}^\dagger |0\rangle\}$ , we introduce fermionic two-component spinors

$$\hat{\Psi}_k = \begin{pmatrix} \hat{c}_k \\ \hat{c}_{-k}^\dagger \end{pmatrix}, \quad \hat{\Psi}_k^\dagger = \begin{pmatrix} \hat{c}_k^\dagger & \hat{c}_{-k} \end{pmatrix}, \quad (\text{A7})$$

allowing us then to write the Hamiltonian of each momentum space block,  $\hat{H}_k$ , in the form

$$\hat{H}_k = 2\Psi_k^\dagger \begin{pmatrix} (\omega - g \cos k) & -ie^{-2i\phi} g \sin k \\ ie^{2i\phi} g \sin k & -(\omega - g \cos k) \end{pmatrix} \Psi_k, \quad (\text{A8})$$

where  $\hat{H} = \sum_{k>0} \hat{H}_k$ . Making the common choice of phase,  $\phi = -\pi/4$ , corresponds to working in the  $x$ - $z$  pseudo-spin basis, allows us to write the Hamiltonian in a more familiar manner viz. the pseudo-spin Pauli matrices as,

$$\hat{H}_k^{spin} = 2\Psi_k^\dagger [(\omega - g \cos k) \sigma_z + (g \sin k) \sigma_x] \Psi_k. \quad (\text{A9})$$

Solving the  $2 \times 2$  eigenvalue problem for the pseudo-spin Hamiltonian provides us with the ground state energy of each momentum-space block,

$$\epsilon_k = -2 \sqrt{g^2 + \omega^2 - 2g\omega \cos k}, \quad (\text{A10})$$

with a corresponding (un-normalised) ground state solution of each block given by

$$|\psi_{GS}\rangle_k = \cos \frac{\theta_k}{2} |0\rangle_k + \sin \frac{\theta_k}{2} |1\rangle_k, \quad (\text{A11})$$

where the angle is defined as  $\tan \theta_k = \frac{\omega \sin k}{\omega \cos k - g}$ . The ground state for an  $N$ -site system is simply given as the tensor product  $|\psi_{GS}\rangle_N = \bigotimes_{k>0} |\psi_{GS}\rangle_k$  of the ground state of each momentum space block  $\hat{H}_k$ . The QFI is additive under tensor product and for a pure state of the form  $|\Psi\rangle = |\psi\rangle_A \otimes |\psi\rangle_B \otimes \dots, |\psi\rangle_N$  can be decomposed as,

$$\mathcal{I}_{\alpha\beta} [|\Psi\rangle_A \otimes |\psi\rangle_B \otimes \dots, |\psi\rangle_N] = \mathcal{I}_{\alpha\beta} [|\psi\rangle_A] + \mathcal{I}_{\alpha\beta} [|\psi\rangle_B] + \dots, \mathcal{I}_{\alpha\beta} [|\psi\rangle_N] \quad (\text{A12})$$

with  $\mathcal{I}_{\alpha\beta} [|\psi\rangle_i]$  defined in Eq. (3). By exploiting the additive property of the QFI under tensor product and the fact that the ground state of a free fermion system can be written as  $|\psi_{GS}\rangle_N = \bigotimes_{k>0} |\psi_{GS}\rangle_k$ , elements of the QFIM can readily be obtained

$$\mathcal{I}_{\alpha\beta} = 4 \sum_k \left[ \langle \partial_\alpha \psi_{GS} | \partial_\beta \psi_{GS} \rangle_k - \langle \partial_\alpha \psi_{GS} | \psi_{GS} \rangle_k \langle \psi_{GS} | \partial_\beta \psi_{GS} \rangle_k \right], \quad (\text{A13})$$



as the sum of the QFI of each momentum space block. Alternatively, the angle  $\theta_k$  containing information regarding the unitary transformation required to diagonalize the system can be used to compute elements of the QFIM viz.,

$$\mathcal{I}_{\alpha\beta} = \sum_k \partial_\alpha \arctan \theta_k \times \partial_\beta \arctan \theta_k. \quad (\text{A14})$$

Equipped with this, the QFIM can readily be obtained for arbitrary system size  $N$  of the TFIM as,

$$\hat{\mathcal{I}} = \sum_k \begin{pmatrix} \frac{g^2 \sin^2 k}{(g^2 + \omega^2 - 2g\omega \cos k)^2} & -\frac{g\omega \sin^2 k}{(g^2 + \omega^2 - 2g\omega \cos k)^2} \\ -\frac{g\omega \sin^2 k}{(g^2 + \omega^2 - 2g\omega \cos k)^2} & \frac{\omega^2 \sin^2 k}{(g^2 + \omega^2 - 2g\omega \cos k)^2} \end{pmatrix}, \quad \text{with } k = \pi(2n+1)/N \text{ and } n = 0, 1, 2, \dots, \frac{N}{2} - 1, \quad (\text{A15})$$

where at the critical point of the TFIM,  $g = \omega$ , elements of the above QFI matrix follow a triangular sequence and coalesce to  $(N^2 + N)/8\omega^2$ . The determinant of the QFIM follows as determinant of the sum of the QFIM of each momentum space block,

$$\det[\hat{\mathcal{I}}] = \det \left[ \sum_k \begin{pmatrix} \frac{g^2 \sin^2 k}{(g^2 + \omega^2 - 2g\omega \cos k)^2} & -\frac{g\omega \sin^2 k}{(g^2 + \omega^2 - 2g\omega \cos k)^2} \\ -\frac{g\omega \sin^2 k}{(g^2 + \omega^2 - 2g\omega \cos k)^2} & \frac{\omega^2 \sin^2 k}{(g^2 + \omega^2 - 2g\omega \cos k)^2} \end{pmatrix} \right], \quad (\text{A16})$$

which in the case of the QFIM is singular for all  $N$ , but in full generality is not strictly singular for any free fermion system and set of parameters.

### APPENDIX C: ADDITIONAL FIGURES

For the sake of clarity, in Figs 1(b) and (f) from the main text, we presented only part of the data used to generate Figs 1(d) and (h). Here we provide all the relevant generated data and plot them in Fig. A2. Note that because of the finite resolution in  $\sigma$ , the red crosses in Figs 1(d) and (h) appear bumpy.

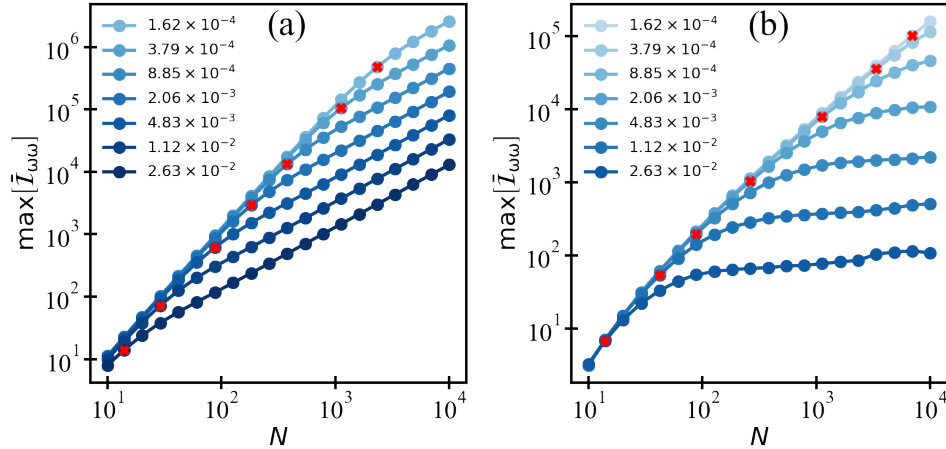


FIG. A2. Scaling of the peak QFI  $\bar{\mathcal{I}}_{\omega\omega}$ , with a given uncertainty  $\sigma/\omega$  in the control parameter  $g$  in shades of blue, as a function of system size  $N$  in the TFIM (a) and LMG (b). Red crosses denote the value at which the QFI feels the uncertainty of the control parameter  $g$  and shows the full compliment of data within the relevant uncertainty range used to generate panels (d) of Fig. 1 and Fig. 1 of the main text.